Collective vector method for the simulation of large atomic $E1$ transition arrays

S. D. Bloom and A. Goldberg
Lawrence Livermore National Laboratory, University of California, Livermore, California 94550
and Department of Applied Science, University of California, Davis, Davis, California 94550
(Received 17 March 1986)

We describe the application of the collective vector method to the evaluation of the moments of atomic transition arrays. We use these moments with the Lanczos algorithm to obtain a Stieltjes δ-function representation of the array. As an example the procedure is applied to a test array containing over 5000 lines in the exact spectrum and is seen to give a good representation of the array with only moderate computational requirements. In comparison the more familiar Gram-Charlier expansion leads to uninterpretable negative excursions making it unusable except for completely unresolved transition arrays.

I. INTRODUCTION

Atomic transition arrays can exhibit large numbers of lines. Those originating from the M shell or above can contain sufficiently large numbers of lines so that detailed microscopic accounting of the lines becomes infeasible. For example, in pure LS coupling the array corresponding to the "source" and "generated" configurations, respectively, $3p^5 3d^4$-$3p^5 3d^3 4f$, contains over 5500 lines and this number increases severalfold in intermediate coupling. (We will use the symbols S and G for the source and generated configurations. Section II gives a fuller discussion as to how these configurations are defined.) Frequently it is unnecessary to account for all these lines since quite often physical broadening mechanisms merge the lines into a continuous strength function, leaving behind a semiresolved structure. If this strength function is totally structureless, as in, e.g., a Gaussian shape, the array is generally termed an unresolved transition array (UTA). Then it suffices to fix only the total strength of the array, its mean frequency, and its width. The UTA concept has been studied by Bauche *et al.*,[1] who have given explicit formulas for the mean frequency and width for a variety of different types of source-generated configuration combinations.

In many other cases, however, although the effective strength function is continuous, the spectrum still shows semiresolved structure (see Fig. 1 in Sec. III). Such a spectrum contains more information than simply the first two moments of the array. In this report, we describe a computational procedure which can be used to describe such semiresolved transition arrays.[2] This procedure is based on the Lanczos algorithm and has been used extensively in treating complex nuclear spectra.[3,4] In the nuclear case one usually considers the transitions as all originating from a single source state, while here one must consider the transitions from a manifold of source states, i.e., those of the source configuration. It is the thrust of this paper to illustrate that the procedure can be profitably applied to this more complex problem, and that one can then obtain with moderate computational efforts detailed information about the semiresolved structure of the transition array.

The prescription has within it two main steps (although in practice the algorithm does not make this separation). For each state in the source manifold one finds a set of moments of the transition array, μ_n, $n=0,1,\ldots,N$, with N chosen as desired. The program then effects a Stieltjes imaging to produce a sharp line spectrum which matches exactly this set of moments. The procedure also produces a width to be associated with each line. The full transition-array strength function is then the sum of the strength functions so produced from each source state.

In Sec. II we outline the details of this procedure and its implementation, and in Sec. III we give results for the test case of the $3d$-$4f$ transition mentioned above. We also show in Sec. III some of the difficulties which arise from the use of the Gram-Charlier expansion[5] to generate the strength function from a finite set of moments of the array.

II. COMPUTATIONAL PROCEDURE

In general the source configuration of the transition array will contain a manifold of states denoted as $\{|S_i\rangle\}$. We consider a prototype state $|S\rangle$ with quantum numbers J_S (total angular momentum), M_J and any other quantum numbers required to specify the source states. We define the collective vector $|CE1;S\rangle$ as follows:

$$|CE1;S\rangle=(E1)|S\rangle\ , \tag{1a}$$

$$(E1)=(E1)_{-1}+(E1)_0+(E1)_1\ , \tag{1b}$$

where $|CE1;S\rangle$ will be represented on the G-configuration space, and $(E1)$ is the one-body electric dipole operator summed over all possible projections $(-1,0,1)$, as shown in Eq. (1b). The use of this summation plus the Wigner-Eckhart theorem leads to the result that all moments are scalars, i.e., independent of spin projection. The configuration space (i.e., the G space) generated by the $E1$ operator, as shown in Eqs. (1a) and (1b), is by convention chosen to be the larger (dimensionally) of the two, since we can, of course, go from either one to the other via the same $E1$ operator. The collective vector has norm N_S, with

$$N_S = \langle CE\,1{:}S \mid CE\,1{:}S \rangle \ , \tag{2}$$

and in fact N_S is the total strength of the array. Note that this whole procedure could be used for the array generated by any multipolar transition by defining the appropriate collective vector. However, here we are concerned only with $E1$ transitions.

While the source state $|\,S\rangle$ is an eigenstate of the atomic Hamiltonian, the collective state $|\,CE\,1{:}S\rangle$ is not, and this is manifested in the nonvanishing of the centroidal moments μ_n defined by

$$\mu_n(S) = \frac{1}{N_S} \langle CE\,1;S \mid [H - \Omega_1(S)]^n \mid CE\,1;S \rangle \qquad n = 2,3,4,\ldots \tag{3}$$

where $\Omega_1(S)$ is the expectation value of the Hamiltonian in the collective vector state,

$$\Omega_1(S) = \frac{1}{N_S} \langle CE\,1;S \mid H \mid CE\,1;S \rangle \ . \tag{4}$$

These $\mu_n(S)$ are the centroidal moments of that part of the transition array originating from the source state $|\,S\rangle$. One also requires the average transition frequency for transitions from that source state, and this is

$$\omega_1(S) = \Omega_1(S) - \langle S \mid H \mid S \rangle \ . \tag{5}$$

It can be shown[2] that Eqs. (3)—(5) are independent of spin projection, as required for scalarity. Evaluation of the array moments can be effected directly from Eqs. (2)—(5). We do this by using the VLADIMIR code. This code is based on the Hausman approach[3] to the Lanczos method and its associated techniques. The alternative approach is described in Ref. 4 where the underlying principles common to both are described, and a review of applications to nuclear reactions is given in Ref. 6. Angular momentum coefficients are not required in the representation of the state vectors in either approach because of the use of Fock-space representation, i.e., occupation number representation, in conjunction with the second-quantized representation for the operators. All symmetries, and hence all angular momentum coupling information, are contained in the coefficients of the operators.[3,4] In the Hausman approach, in contrast to the alternative, the method of second quantization is used at all stages, so that, for example, the operation in Eqs. (1a) and (1b) is accomplished by actual computer operation of the sum of three operators on the source vector $|\,S\rangle$ to yield a new state vector $|\,CE\,1\rangle$. In particular, the state vectors are represented by linear combinations of Slater determinants (or basis vectors) with associated amplitudes. Each Slater determinant, in turn, is represented by a binary word with (0,1) in each bit designating (unoccupied,occupied) orbitals in m-space. The second-quantized operators are stored in multidimensional arrays, two dimensional for one-body operators, four dimensional for two-body operators, etc.[7] These entities, i.e., the operators and the state vectors, can be used in any arbitrary combination or sequence to produce new state vectors. Similarly, scalar products of arbitrary state vectors as in Eq. (3) can be generated by straightforward multiplication using the standard vector functions of computers such as the CDC7600 or the CRAY series.

In the second part of this procedure we use the moments calculated as described above to explicitly construct a synthesis of the transition-array strength function $S(\omega)$. Since each source state $|\,S\rangle$ with angular momentum J_S is $(2J_S+1)$-fold degenerate, the mean frequency and the centroidal moments of the entire array are

$$\omega_1 = \sum_S (2J_S+1)\omega_1(S) \ , \tag{6a}$$

$$\mu_n = \sum_S (2J_S+1)\mu_n(S) \ . \tag{6b}$$

One widely used method of using these moments to synthesize the strength function is as an expansion in Hermite polynomials, via the Gram-Charlier expansion,[5] i.e.,

$$S(\omega) = \frac{2}{\pi} \sum_n c_n \exp[-(\omega-\omega_1)^2/2\mu_2] H_n[(\omega-\omega_1)/\sqrt{\mu_2}] \ . \tag{7}$$

This expansion, exact if carried to infinite order, as a practical matter is truncated at $n=N$, with the coefficients $c_0, c_1, \ldots, c_N$ chosen so as to ensure that $S(\omega)$ correctly gives the first $N+1$ centroidal moments ($\mu_0=1, \mu_1=0$). Keeping only the terms through $N=2$ gives a Gaussian strength function, that used in Ref. 1. We show in Sec. III, however, that extension of the expansion to N beyond 2 presents serious difficulties, to wit that the manifestly positive definite $S(\omega)$ is simulated by a function which can and indeed does exhibit negative values and that these physically unacceptable negative excursions can be significant.

A second possible route, and the one we use, is the Stieltjes imaging or δ-function expansion, implemented through the Lanczos algorithm. For each source state $|\,S\rangle$, one constructs from the collective vector $|\,CE\,1{:}S\rangle$ a set of N vectors ζ_n by

$$\zeta_n = H^{n-1} \mid CE\,1{:}S \rangle \ , \quad n = 1,2,\ldots,N \ , \tag{8}$$

and in this N-dimensional space one then diagonalizes the Hamiltonian H to obtain the N eigenvectors χ_n and associated eigenvalues η_n. To each of these eigenvectors there then corresponds a sharp line in the transition array at frequency η_n with relative intensity

$$\lambda_n = |\,\langle \chi_n \mid CE\,1{:}S \rangle\,|^2 \ .$$

It can be shown[8] that the N sharp lines generated by this procedure gives a δ-function representation of the strength function whose first $2N-1$ centroidal moments exactly match those of the true strength function. Iteration of the procedure to $N=6$ gives correctly the first 11 moments for that source state. The full transition-array strength function is, of course, synthesized by following this recipe for all source states to give a set of $N \times N_S$ (N_S is the number of source states) sharp lines in toto. As will be seen in Sec. III, six iterations per source state generates a quite accurate mimic of the full transition array, and even only one iteration per source state gives a good picture of the strength function.

In order to display these results it proves necessary to provide each of these lines with a width and with a profile function of some form. It should be noted that ascribing, for example, a Gaussian shape with finite width to each line alters the moments. But as will be seen the change is not significant so long as the individual line widths are small compared to the width of the main structural features within the array. It is also possible to assign a width to each line on the basis of the computation itself. Since the state vectors χ_n are not eigenvectors of H in the G space, but only in the restricted N-dimensional space (N being the number of iterations), these approximate eigenvectors have a variance in their energy,

$$\Gamma_{Ln}^2 = \langle \chi_n | H^2 | \chi_n \rangle - \langle \chi_n | H | \chi_n \rangle^2 . \quad (9)$$

We note that Γ_{Ln} is entirely a mathematical artifact of the Lanczos algorithm, in that it represents the spread in the state vector χ over the true state vectors of the G multiplet. With increasing N, Γ_{Ln} decreases, and at N equal to the total number of states in the G multiplet this computational width vanishes, i.e., one achieves a full diagonalization of the G manifold. Note that these widths, just as in the case of an arbitrary width discussed above, alter the moments. Nonetheless, the rendering of the shape of the spectrum is, in general, significantly improved by using this "computational" width, as will be shown.

III. APPLICATION TO A TEST CASE

We have applied this procedure to the transition array corresponding to

$$3p^5 3d^4 - 3p^5 3d^3 4f .$$

Without spin-orbit interaction, this array contains 5523 distinct transition lines. The Hamiltonian H is taken as the set of one-body terms arising from the single-particle energies including the perturbation correction due to the interaction with the core, and a set of two-body terms resulting from the repulsion between valence electrons, given in terms of standard Slater integrals. These are all taken in the one-electron basis states $| n,l,j,m_j \rangle$. The Hamiltonian matrix elements are taken from a Hartree-Slater calculation[9] for Fe VI,[9] and have been used for both an exact microscopic transition array and for the methods outlined above. (The only other datum required for the array is the one-electron dipole integral, which provides an overall scale factor for the array.)

In Fig. 1 we show the microscopic transition array, generated from an intermediate coupling code.[10] (This code can include spin-orbit interaction, although none was utilized here.) In these figures we have, as described above, endowed each sharp line with a Gaussian profile of width Γ_x, with Γ_x taken as indicated. Table I shows the mean frequency and the centroidal moments about this mean up to $n=24$.

We have used Eqs. (1)—(6) through six iterations to generate six moments per source state and thereby the first six moments of the full array (beyond the overall strength which can be scaled out). The first of these is the mean frequency ω_1, and then finally μ_2 through μ_6. These values are listed in Table I and agree, as they should, quite well with the microscopically calculated moments.

If we use these six correct moments to generate $S(\omega)$ via the Gram-Charlier expansion via Eq. (7), truncated at $N=6$, we can then compute a set of moments beyond the sixth and these are listed also in Table I in Column II. Beyond the sixth moment these values differ from the true moments with errors of approximately 10% up to the 12th, where the errors become larger, of order 100%. The use of the Gram-Charlier expansion as a representation of the array, however, is misleading as can be seen from the plot of $S(\omega)$ in Fig. 2 showing negative excursion of the strength function so that the tails of the strength function are without physical meaning. In addition to this rather undesirable feature, such an expansion with this few moments cannot give any details of any structure in the transition array, even that in Fig. 1(b) which is overlaid in Fig. 2. In order to obtain such structure via this expansion would require N approximately 25, and this was establish-

TABLE I. Computed centroidal moments μ_n of transition array. (The numbers in square brackets give the power of ten by which the numbers are to be multiplied.) Column I gives the centroidal moments μ_n, $n=2$—24 for the exact microscopic array, Column II those computed from the Gram-Charlier expansion with six iterations per source state, Columns III and IV those computed from the delta expansion with six iterations and with one iteration per source state, respectively. ω_1 in each column is the centroidal energy. In Columns II, III, and IV the moments above the asterisks should agree with the microscopic moments, while those below are then extrapolated from the correct moments according to the methods described in the text.

n	Column I $\omega_1=$ 195.45	Column II $\omega_1=$ 195.44	Column III $\omega_1=$ 195.45	Column IV $\omega_1=$ 195.48
2	3.70[1]	3.70[1]	3.70[1]	3.70[1]
				***
3	2.66[2]	2.67[2]	2.67[2]	1.69[2]
4	8.27[3]	8.27[3]	8.29[3]	6.56[3]
5	1.37[5]	1.37[5]	1.37[5]	0.77[5]
6	3.72[6]	3.72[6]	3.74[6]	2.56[6]
7	7.79[7]	6.79[7]	7.81[7]	4.51[7]
8	2.15[9]	2.07[9]	2.16[9]	1.55[9]
9	5.01[10]	3.68[10]	5.04[10]	3.46[10]
10	1.43[12]	1.29[12]	1.44[12]	1.25[12]
11	3.59[13]	2.22[13]	3.60[13]	3.30[13]
12	1.06[15]	0.88[15]	1.07[15]	1.24[15]
			***	
13	2.82[16]	1.48[16]	2.83[16]	
14	8.64[17]	6.61[17]	8.70[17]	
15	2.43[19]	1.11[19]	2.44[19]	
16	7.74[20]	5.37[20]	7.77[20]	
17	2.29[22]	0.91[22]	2.29[22]	
18	7.53[23]	4.71[23]	7.53[23]	
19	2.33[25]	0.82[25]	2.32[25]	
20	7.89[26]	4.42[26]	7.84[26]	
21	2.53[28]	0.81[28]	2.51[28]	
22	8.75[29]	4.43[29]	8.64[29]	
23	2.89[31]	0.87[31]	2.84[31]	
24	1.01[33]	0.47[33]	0.99[33]	

ed only *a posteriori*. For $N > 25$ the expansion exhibits extremely large negative excursions. The Lanczos procedure, carried to six iterations, produces a sharp line strength function $S(\omega)$ with correct moments up to the 12th. This can be used to generate higher moments and the results up to the 24th moment are listed in the last column of Table I. These additional computed moments are quite accurate and even the worst of these μ_{24} has an error of only 2%.

The array from this six-iteration δ expansion is shown in Fig. 3, with each line given an equal width $\Gamma = 0.25$ eV as indicated. Figure 3(b) shows the overlay of these results with the microscopic array of the same width, that in Fig. 1(a). Overall, the general structure of the microscopic array is reproduced by this six-iteration calculation, as was evidenced by the good agreement in the moments in Table I.

In Fig. 4 we show the same results, except that here each line is given a width equal to the greater of the two, that from Eq. (9) or 0.25 eV. We also show in Fig. 4 the overlap of this with the broadened microscopic array.

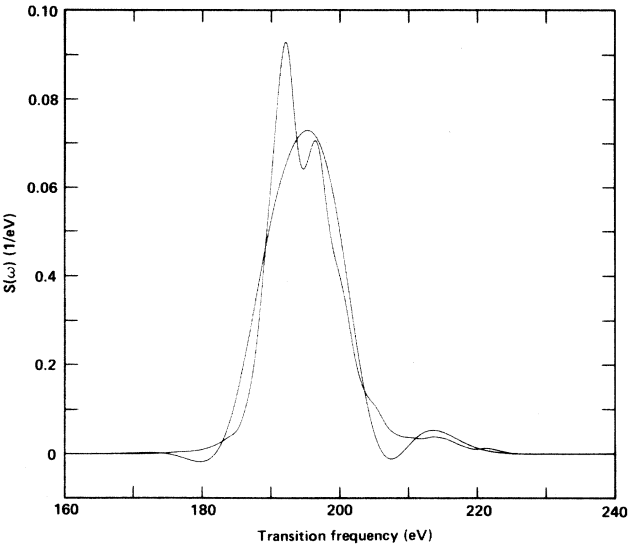

FIG. 2. Overlay of the microscopic spectrum with $\Gamma_x = 1$ eV and the GC (Gram-Charlier) expansion with six moments. The GC spectrum is negative in the tails of the distribution, giving an unphysical spectrum. Furthermore, the double-humped structure at the center does not appear at all in the GC result.

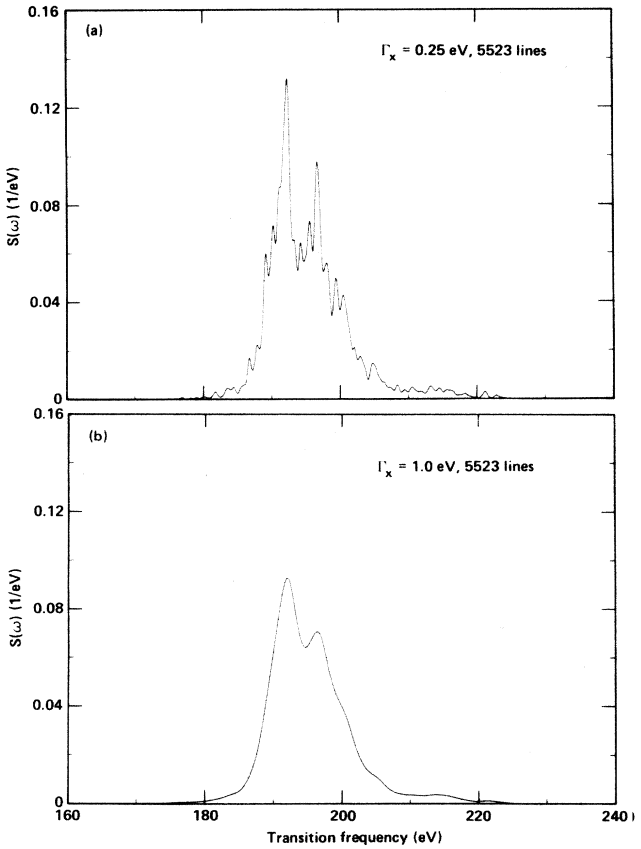

FIG. 1. (a) Microscopic spectrum for $3p^5 3d^4$-$3p^5 3d^3 4f$ array. A Gaussian line shape of width $\Gamma_x = 0.25$ eV has been assigned to each of the 5523 lines of this spectrum, averaging out much of the structure. The remaining structure is termed semiresolved. (b) Same as (a) except with $\Gamma_x = 1$ eV. The highly smoothed spectrum still reveals semiresolved structure in the non-Gaussian tails and also in the double peak in the middle of the spectrum.

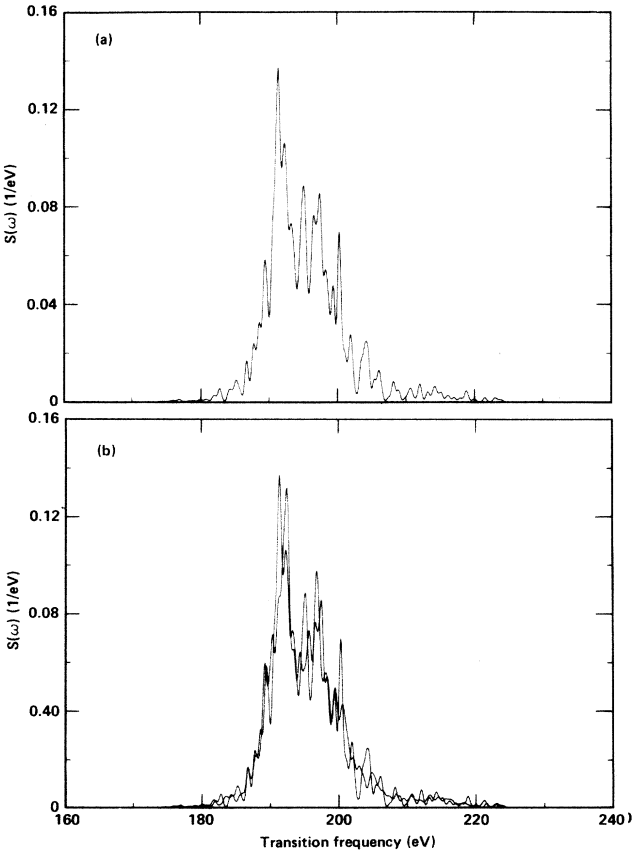

FIG. 3. (a) Lanczos δ-expansion for six iterations per source state. Each sharp line has been assigned a width of 0.25 eV. Since the source configuration has 180 states in toto, this represents the microscopic spectrum (5523 lines) by 1080 lines. (See Sec. II.) (b) Overlay of the microscopic spectrum [Fig. 1(a)] and the above Lanczos spectrum [Fig. 3(a)].

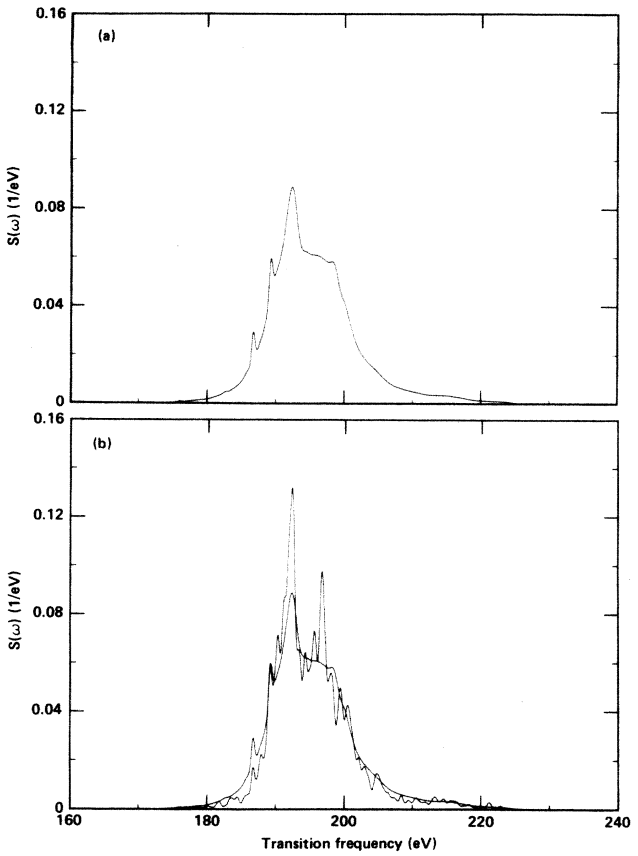

FIG. 4. (a) Lanczos δ-expansion with six iterations per source state. The widths are taken as the greater of 0.25 eV or the intrinsic computational width (Sec. II). (b) Overlay of Fig. 3(a) and the microscopic spectrum with 0.25 eV width.

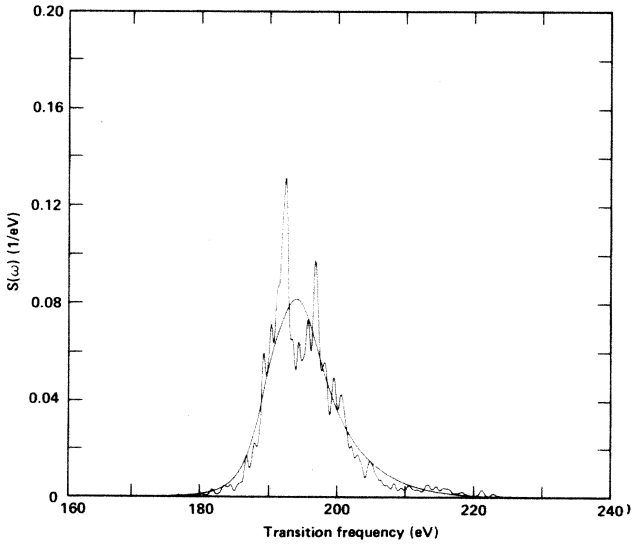

FIG. 5. Overlay of the Lanczos δ-expansion with one iteration per source state and with computational width and the microscopic spectrum of Fig. 1(b).

Use of this computational width essentially washes out some but not all of the intermediate structure features.

Finally, we note that the simplest Lanczos procedure with *only one iteration per source state* produces an array with the correct first two moments. One can expect that here use of the computational width would produce effectively an unresolved array and indeed that is the case, as shown in Fig. 5. It is apparent, however, that the result is not a pure Gaussian strength function, but also possesses a skewness matching that of the true array. In fact, up to the 12th moment the average deviation from the exact values is only about 25% (see Table I).

IV. DISCUSSION AND CONCLUSIONS

We have shown here that the construction of a collective $E1$ state vector from each of the parent states of a transition array provides a compact basis for obtaining, via the Lanczos δ expansion, an excellent approximation to the strength function of that array. There are no restrictions in this approach such as the requirement of LS coupling, etc. In lowest order the method leads to one line per source state vector, which in our example results in 180 lines representing the 5523 lines in the true array. In this case the first two moments are rigorously correct but the succeeding moments up to the 12th differ from the correct values on the average by only 25%. In the highest approximation studied here, i.e., six iterations per source state, the semiresolved structure of the microscopic spectrum, which shows up at a resolution of 0.25 eV for each line, is quite well reproduced. Here we use 1080 lines to represent the full number in the microscopic array, and we find that the moments accurately reproduce the correct values up to the 24th, although only the first 12 are rigorously correct. Hence this procedure can approximately represent complex spectra with semiresolved structure with a line structure only a fraction of the full size of the array.

The Gram-Charlier (GC) expansion, expressed as Hermite polynomials with a Gaussian weighting, requires, as noted earlier, in the range of 25 moments to reproduce any of this semiresolved structure. The negative excursions inherent in this method, however, make a physical interpretation of the results impossible. (In fact, we have found that this difficulty is already present with only three moments of information.) The conclusion then is that this GC method is appropriate only when no more than the centroid and width are required, i.e., the case of a totally unresolved array (UTA).

We summarize here the advantages of the collective-vector—Lanczos approach to studying transition-strength distributions.

(1) As noted in Ref. 4, the Lanczos method leads to a very compact, essentially one-dimensional, representation for the system Hamiltonian.

(2) The collective state vector contains all necessary information about the transition array. The Hamiltonian decomposition of the collective vector via the Lanczos algorithm leads to a synthesis of the transition array, replacing it with another much smaller array, 2—20% of the original, but which retains rigorously the correct mo-

ments for the full array up to the $2n$th moment, where n is the number of Lanczos iterations. Even moments beyond this are reproduced with high accuracy.

(3) The inclusion of configuration mixing requires nothing more than the specification of the Hamiltonian matrix elements between the single particle states of the different configurations. The program would then require neither more computer memory nor time.

(4) Transition arrays for higher multipoles, e.g., $E2$, are no more difficult than the $E1$ array studied here. The only practical limitation results from the computer memory required for the generated configuration or G space. The model calculation illustrated here used only 10% of the available memory.

(5) Perhaps the most important advantage is that transition arrays with the same source configuration but with much more complex generated configurations require essentially no further computational effort, so that one could also deal with transition arrays with many more states in the generated configuration and correspondingly many more in the array. In such cases, microscopic spectra would be beyond the capabilities of available computers.

Where semiresolved structure is of interest and where a full treatment of the complete microscopic array is impractical or even uninteresting, the Lanczos δ-expansion method is a reliable scheme for obtaining the essential features with a representative set of lines whose number is a relatively small fraction of the total, typically 3—20%. This scheme itself becomes impractical when the number of source states is large (e.g., approximately 1000) and other methods are required. We are pursuing a Monte Carlo scheme for representing the source manifold and then applying the Lanczos δ procedure as described here. This approach could cut down the size of the required source manifold by an order of magnitude or more.

ACKNOWLEDGMENTS

We are grateful to S. M. Grimes and also to J. D. Anderson for several enlightening conversations. This work was performed under the auspices of the U.S. Department of Energy by Lawrence Livermore National Laboratory under Contract No. W-7465-Eng-48.

[1]C. Bauche-Arnoult, J. Bauche, and M. Klapisch, Phys. Rev. A **20**, 2424 (1979); J. Bauche *et al.*, *ibid.* **28**, 829 (1983).

[2]S. D. Bloom and A. Goldberg, in Proceedings of the 3rd International Conference on Radiative Properties of Hot Dense Matter, Williamsburg, Virginia, 1985 (unpublished) [Lawrence Livermore National Laboratory Report No. UCRL-93608, 1985 (unpublished)].

[3]R. F. Hausman, Lawrence Livermore National Laboratory Report No. UCRL-52178, 1978 (unpublished).

[4]R. R. Whitehead, A. Watt, B. J. Cole, and I. Morrison, Adv. Nucl. Phys. **9**, 123 (1977)

[5]M. Kendall and A. Stuart, *The Advanced Theory of Statistics* (MacMillan, New York, 1977), pp. 168—175.

[6]S. D. Bloom, *Progress in Particle and Nuclear Physics,* edited by D. H. Wilkinson (Wheaton, London, 1983), Vol. 11, p. 585.

[7]See, e.g., A. deShalit and H. Feshbach, *Theoretical Nuclear Physics* (Wiley, New York, 1974), Ch. VII.

[8]B. F. Rozsnyai, private communication.

[9]A. Goldberg, B. F. Rozsnyai, and P. Thompson, Phys. Rev. A **34**, 421 (1986).

[10]R. R. Whitehead, *Moment Methods in Many-Fermion Systems,* edited by B. J. Dalton, S. M. Grimes, J. P. Vary, and S. A. Williams (Plenum, New York, 1979), p. 81.